Molecular Therapy
Methods & Clinical Development
Original Article

Model for predicting age-dependent safety and immunomodulatory effects of STING ligands in non-human primates

Shokichi Takahama,[1] Kazuya Ishige,[2] Takuto Nogimori,[1] Yasuhiro Yasutomi,[3] Victor Appay,[1,4] and Takuya Yamamoto[1,5,6,7]

[1]Laboratory of Immunosenescence, Center for Vaccine and Adjuvant Research, National Institutes of Biomedical Innovation, Health and Nutrition, 7-6-8, Saito-Asagi, Ibaraki City, Osaka 567-0085, Japan; [2]Biochemicals Division, Yamasa Corporation, Chiba 288-0056, Japan; [3]Laboratory of Immunoregulation and Vaccine Research, Tsukuba Primate Research Center, National Institutes of Biomedical Innovation, Health and Nutrition, Ibaraki 305-0843, Japan; [4]Université de Bordeaux, CNRS UMR 5164, INSERM ERL 1303, ImmunoConcEpT, 33000 Bordeaux, France; [5]Laboratory of Aging and Immune Regulation, Graduate School of Pharmaceutical Sciences, Osaka University, Osaka 565-0871, Japan; [6]Department of Virology and Immunology, Graduate School of Medicine, Osaka University, Osaka 565-0871, Japan; [7]Laboratory of Translational Cancer Immunology and Biology, Next-generation Precision Medicine Research Center, Osaka International Cancer Institute, Osaka 541-8567, Japan

Stimulator of interferon genes (STING) is a cytoplasmic dinucleotide sensor used as an immunomodulatory agent for cancer treatment. The efficacy of the STING ligand (STING-L) against various tumors has been evaluated in mouse models; however, its safety and efficacy in non-human primates have not been reported. We examined the effects of escalating doses of cyclic-di-adenosine monophosphate (c-di-AMP) or cyclic [G (3′,5′)pA (3′,5′p] (3′-3′-cGAMP) administered intramuscularly or intravenously to cynomolgus macaques. Both ligands induced transient local and systemic inflammatory responses and systemic immunomodulatory responses, including the up-regulation of interferon-α (IFN-α) and IFN-γ expression and the activation of multiple immunocompetent cell subsets. Better immunological responses were observed in animals that received c-di-AMP compared with those that received 3′-3′-cGAMP. Multi-parameter analysis using a dataset obtained before administering the ligands predicted the efficacy outcome partially. Importantly, the efficacy of these ligands was reduced in older macaques. We propose that 0.5 mg/kg c-di-AMP via intramuscular administration should be the optimal starting point for clinical studies. Our study is the first to demonstrate the age-dependent safety and efficacy of STING-L in non-human primates and supports the potential of STING-L use as a direct immunomodulator *in vivo*.

INTRODUCTION

Pattern recognition receptors (PRRs) detect various pathogens and damage-associated molecular patterns and provide a link between innate and adaptive immunity.[1] As PRR activation triggers signaling cascades and activates both the innate and adaptive immune systems, PRR ligands are used as vaccine adjuvants or immune modulators in the treatment of infectious diseases and cancer.[2,3] To date, approximately 20 PRRs have been reported. Among them, we focused on stimulator of interferon genes (STING, also known as MPYS/MITA/ERIS/TMEM173), as STING ligands are one of the best candidates for producing type I interferon (IFN) and IFN-γ *in vitro*.[4]

STING is an endoplasmic reticulum-associated PRR that serves as a sensor of cytoplasmic cyclic dinucleotides (CDNs).[5–8] STING is expressed ubiquitously[6–8] and plays an essential role in defense against DNA viruses or bacterial pathogens. Experiments using *Sting*-knockout (KO) mice have shown that STING is essential for type I IFN production.[9] Furthermore, vaccine-induced cytotoxic T cell (CTL) responses were reduced in these mice,[9] indicating that STING is essential for inducing the CTL response.

STING activation is triggered in response to CDN—for example, cyclic [G (3',5')pA (3',5')p] (commonly known as 2'-3'-cGAMP) is produced in response to the activation of cyclic GMP-AMP synthase (cGAS)—binding.[6,10–12] The binding of STING to cGAMP results in the release of type I IFN via NF-κB activation and TANK binding kinase 1 (TBK1)-mediated phosphorylation and the subsequent nuclear translocation of interferon regulatory factor 3 (IRF-3).

Various agonists have been used to delineate the molecular mechanisms underlying the cGAS–STING axis. 2'-3'-cGAMP is considered a natural STING ligand (hereafter referred to as STING-L) in human cells, and bacterial CDNs such as c-di-AMP and c-di-GMP that structurally resemble cGAMP also serve as STING-Ls.[5,13] 3'-3'-cGAMP and c-di-AMP have been reported to activate STING in human,[14,15]

Received 22 July 2022; accepted 12 December 2022;
https://doi.org/10.1016/j.omtm.2022.12.008.

Correspondence: Takuya Yamamoto, Laboratory of Immunosenescence, National Institutes of Biomedical Innovation, Health and Nutrition, 7-6-8, Saito-Asagi, Ibaraki City, Osaka 567-0085, Japan.
E-mail: yamamotot2@nibiohn.go.jp

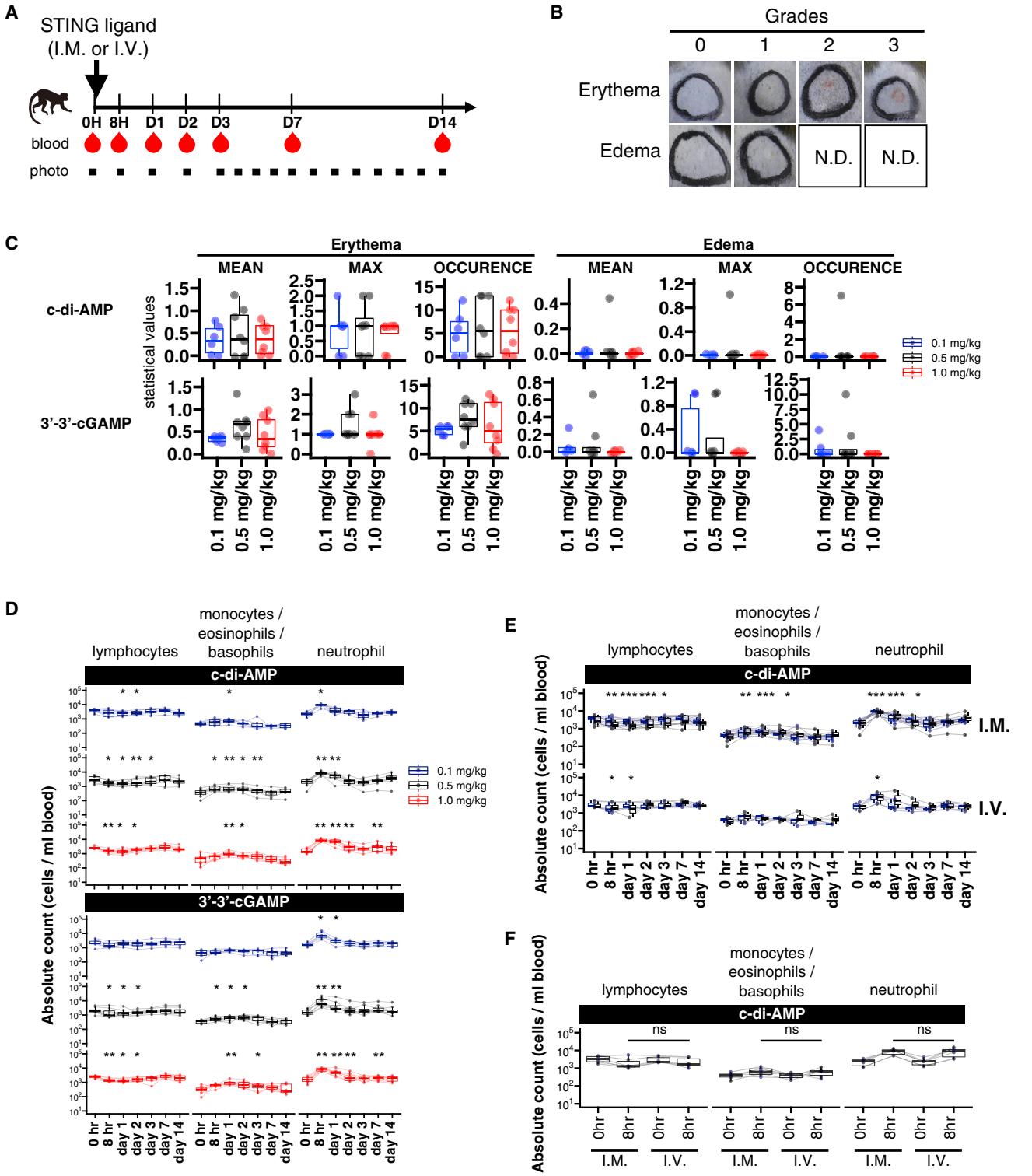

Figure 1. Safety assessment for the *in vivo* administration of STING ligands

(A) Schematic depiction of the experimental schedule. Cynomolgus macaques were administered with different doses of STING-L (either c-di-AMP or 3'-3'-cGAMP) intramuscularly. (B) Representative images for the inflammatory response at the local administration site. Grades were determined using the criteria described in the materials and methods section. (C) Statistical values of scoring in each dosing group are shown. The terms mean, max, and occurrence indicate the mean and maximum scores, and the

(legend continued on next page)

rhesus monkey, and cynomolgus macaque peripheral blood mononuclear cells (PBMCs) *in vitro*.[4,16] In addition to mammals, diverse species express STING; these include zebrafish, frogs, fruit flies, sea anemones, and bacteria.[17] However, some ligands exhibit species-specific properties. For example, murine STING-L DMXAA and its derivative CMA can activate rodent STING, but not human STING.[18,19]

The intratumoral administration of synthetic CDNs has been reported to induce tumor regression at both primary and metastatic sites and stimulate the recruitment of tumor-specific CD8 T cells.[20] Therefore, STING has been recognized as an attractive target for treating tumors.[21,22] Thus, STING-Ls can serve as potent immunotherapeutic agents, and various types of STING-Ls have been examined in clinical trials.[23]

Although the activity of the cGAS-STING axis is rigidly controlled by a negative-feedback loop,[24] sustained STING activation results in lethal STING-dependent proinflammatory diseases in mice[25,26] and autoimmune diseases in humans.[27–29] Thus, an analysis of the safety of *in vivo* STING-L administration using clinically relevant animal models, such as non-human primates (NHPs), is an important first step to harnessing these ligands for clinical therapies. However, the safety and efficacy of a single intratumoral dose or the systemic administration of STING ligands *in vivo* have been studied primarily in mice.[20,30] In this respect, NHPs are highly useful preclinical models as their physiological properties and susceptibility to diseases are more similar to humans than those in rodents.[31,32] Furthermore, macaques show greater within-species genetic diversity than genetically uniform mouse models, enabling analysis of individual differences induced during the treatment. Given the therapeutic potential of STING-Ls, a relevant model to study STING-L-induced cellular responses in humans is required. However, the outcome of STING-L administration to NHPs is limited to only a few reports.[33,34] Therefore, we aimed to investigate the potential of STING-Ls as direct immunomodulators using an NHP model.

RESULTS

Reactogenicity of single-dose administration of STING-Ls to cynomolgus macaques

Cynomolgus macaques were administered STING-Ls (c-di-AMP or 3'-3'-cGAMP) via the intramuscular (i.m.) route. Follow-up was performed for 14 days with blood sampling, and the local adverse responses at the administration site were recorded using photographs and evaluated visually using a five-grade-point scale (Figures 1A, 1B, and S1A). No grade 4 adverse effects were observed in the examined macaques (Figures S1B and S1C). Scoring indicated minimal or mild inflammatory responses at the administration site, which emerged 8 h to 7 days post-administration (8 hpa to 7 dpa; Figures S1B and S1C). However, these responses gradually subsided within 2 weeks. Erythema was observed in most cases, although the severity of the phenotype was mostly minimal or mild. In contrast, edema was observed in five macaques, and no macaque had a score greater than grade 2 over 14 days. There were no statistically significant differences between the dosage groups (Figure 1C), indicating that the magnitude and occurrence of edema and erythema depend on the individual macaque background rather than the dose administered for a range of 0.1–1.0 mg/kg.

After the administration of STING-Ls, neutrophil counts detected by complete blood counts (CBCs) began to increase at 8 hpa and subsequently returned to the baseline within 3–7 days (Figures 1D and S1D). Conversely, lymphocyte counts decreased at 8 hpa and returned to baseline within 3–7 dpa when using either ligand. These systemic inflammatory responses were independent of the ligand type. Similar responses were observed between dose groups, and the magnitude of the response did not change in a dose-dependent manner (Figures 1D and S1D).

To compare the administration routes, three macaques were treated via the intravenous (i.v.) route with 0.1 or 0.5 mg/kg STING-Ls. As observed with the i.m. route, the i.v. route also resulted in the transient upregulation of neutrophils and concomitant reduction in lymphocytes, but these values returned to baseline within 14 days (Figure 1E). There was no significant difference in absolute counts for each subset at 8 hpa between i.m. and i.v. routes (Figure 1F).

Systemic cytokine release triggered by single-dose STING-L administration

We examined the levels of proinflammatory cytokines in the plasma. Levels of IL-1RA and IL-6 began to increase at 8 hpa and gradually declined after that (Figures 2A and 2B). Scoring and CBC data revealed the absence of a clear dose dependency; however, the significant upregulation of IL-1RA or IL-6 levels at 8 hpa was not observed when using 0.1 mg/kg c-di-AMP. This suggested that the effect of STING-Ls on proinflammatory cytokines was dose dependent between doses of 0.1 and 0.5 mg/kg; however, no significant difference was observed using a dose greater than 0.5 mg/kg. These results indicate that the i.m. administration of STING-L is safe up to a concentration of 1.0 mg/kg in cynomolgus macaques.

Next, to investigate the immunological benefits of STING-L administration, we evaluated the plasma levels of cytokines with

number of observations for each macaque over 14 days, respectively. The score differences between the groups were not statistically significant. (D) Variations in the absolute counts of small (lymphocytes), medium (monocytes/eosinophils/basophils), and large-sized cells (neutrophils) are shown. Data were obtained from the complete blood counts of the c-di-AMP (top) or the 3'-3'-cGAMP group (bottom) after the intramuscular (i.m.) administration of STING ligands. The blue, black, and red dots and the lines indicate the 0.1, 0.5, and 1.0 mg/kg doses, respectively. (E) Variations in the absolute counts of small (lymphocytes), medium (monocytes/eosinophils/basophils), and large-sized cells (neutrophils) are shown. Data were obtained from the complete blood counts of the i.m. (top) or intravascular (i.v.; bottom) administration of c-di-AMP. The blue and black dots and the lines indicate the 0.1 and 0.5 mg/kg doses, respectively. (F) Comparison of i.m. with i.v. administration at 8 h post-administration. *p* values were calculated by Wilcoxon signed-rank test (D-F, 0 hr vs each timepoint) and by Kruskal-Wallis test (C). Statistical significance is indicated using * for the values $*p < 0.05$ and $**p < 0.01$.

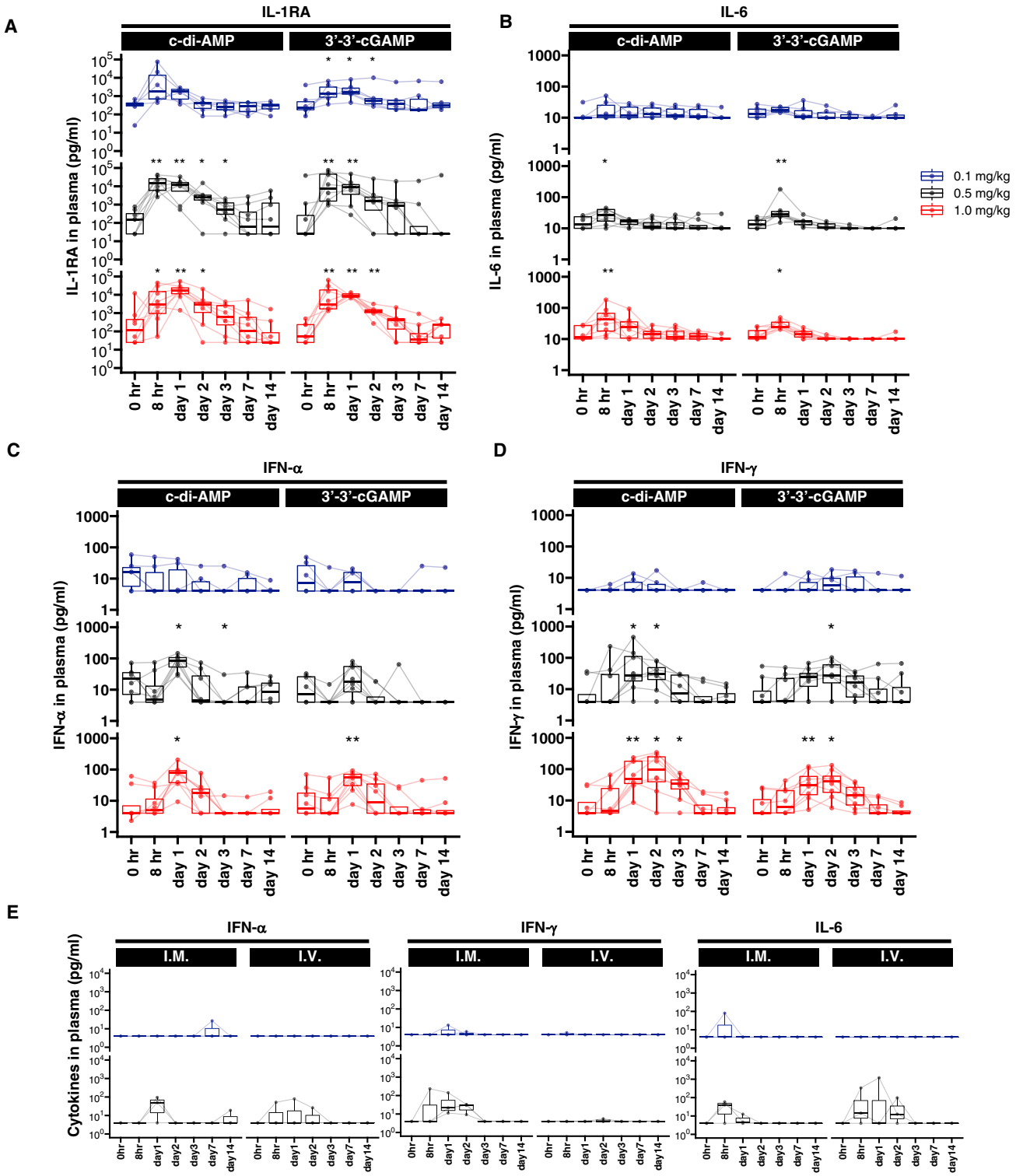

Figure 2. Changes in the level of plasma cytokines post-STING ligand administration

(A–D) Graph of the kinetics of IL-1RA (A), IL-6, (B) IFN-α (C), and IFN-γ (D) levels in plasma after the intramuscular administration of STING ligands. *p* values were calculated by Wilcoxon signed-rank test (0 hr vs each timepoint). Statistical significance is indicated using * for the values $*p < 0.05$ and $**p < 0.01$. (E) Comparison of the changes in plasma cytokine levels between intramuscular (i.m.) and intravenous (i.v.) routes. The blue, black, and red dots and the lines indicate the 0.1, 0.5, and 1.0 mg/kg doses respectively.

immunomodulatory functions. IFN-α levels increased at 1 dpa and subsequently returned to baseline in macaques treated with >0.5 mg/kg c-di-AMP (Figure 2C). A similar increase was observed in the 3'-3'-cGAMP-treated group; however, significant differences were only observed with the highest dose (1.0 mg/kg). Likewise, a dose of >0.5 mg/kg STING-L increased plasma IFN-γ levels at 1 dpa (Figure 2D). The induced levels of IFN-α and IFN-γ were approximately 100 pg/mL, which was higher than those induced by CpG-DNA (K3) or poly(I:C), as previously reported.[35] These results indicated that a dose of 0.5 mg/kg STING-L is required to induce detectable plasma levels of functional cytokines such as IFN-α or IFN-γ in macaques.

We also examined the route-dependent induction of functional cytokines by STING-Ls (Figure 2E). Compared with that with i.m. administration, no IFN-γ was induced by i.v. administration (Figure 2E middle). Further, IL-6 expression was higher and broadly induced by i.v. administration (Figure 2E right). This led to the conclusion that the i.m. route is more appropriate than the i.v. route for the induction of functional cytokines without inducing sustained proinflammatory cytokines.

We next performed correlation analyses (Figure S2) to examine the relationships between cytokines. The correlation matrix indicated several correlations between cytokines at 8 h to 1 dpa (Figure S2A). In particular, we observed correlations between the levels of IL-1RA and IL-6 (Figure S2B) and IFN-α and IFN-γ at 1 dpa (Figure S2C). Of note, correlations between the levels of IL-6 at 8 hpa and IFN-γ at 1 dpa suggested that preceding IL-6 induction potentially contributes to the induction of IFN-γ (Figure S2D).

Effect of single-dose STING-L administration on monocytes and dendritic cell (DC) subsets

Next, we examined the effect of STING-L on the frequency and phenotypes of the PBMC subsets by multicolor flow cytometry. We and others previously described the effect of PRRs on monocytes in cynomolgus macaques.[35] Accordingly, we examined the effects of STING-Ls on monocytes. The counts of intermediate monocytes (iMos) —defined by the expression of CD14 and CD16— increased transiently at early time points (day 1–2) and subsequently returned to the baseline within 7 days (Figures 3A, 3B, S3A, and S3B). The expression of CD169/Siglec-1, an activation marker,[36] was upregulated at 1 dpa and returned to baseline on day 7 (Figures 3C, 3D, and S3C). The change in monocyte composition and activation of iMos after STING-L administration indicated the presence of transient inflammatory responses, as indicated by CBCs and ELISA.

Recently, human CD169+ classical monocytes (cMos) were found to express greater levels of co-stimulatory molecules, relative to those in CD169-negative monocytes, and boost antigen presentation to CD8 T cells.[37] To examine the co-stimulatory molecule expressed on CD169+ monocytes of cynomolgus macaques, we compared the expression of CD80 between the CD169+ and CD169− subsets at 1 dpa. The frequency of CD80-positive cells was increased in the CD169+ cMo or iMo (Figure 3E) groups compared with that in the CD169− counterparts, indicating that these subsets may contribute to the activation of CD8 T cells.

Circulating DCs are the main producers of IFN-α in blood. Therefore, we investigated myeloid/conventional DC (mDC) and plasmacytoid DC (pDC) activation in response to STING-L administration (Figure S3A). Increased surface expression of CD80 in mDCs was detected at 8 hpa in the c-di-AMP-treated group and at 1 dpa in the 3'-3'-cGAMP-treated group (Figures 3F and S3D). The activation of pDCs was also observed in some macaques, though significant differences were not observed except at 2 dpa in the 0.5 mg/mg c-di-AMP-treated group. As DCs show some transient level of activation, they may contribute to the IFN-α production measured in blood. Although we do not have immunohistochemical data, a local *in situ* search for IFN-α by immunohistochemistry would help decipher the cell type that contributes to its production more precisely.

We generated a correlation matrix to assess the relationship between the activation of DC/monocyte subsets and cytokine production (Figure S3E). Of note, we found correlations between the percentage of CD169+ cells in monocytes and the levels of IL-1RA or IL-6 at 1 dpa (Figure S3F), suggesting that the induction of inflammatory cytokines potentially depends on monocyte activation. Although correlations between CD80 expression in DC subsets and the levels of IFN-α were not observed, CD40 expression in DCs at 8 hpa was positively correlated with IFN-α levels, suggesting that DC activation could contribute to the induction of type I IFN (Figure S3G).

Effect of single-dose STING-L administration on T and NK lymphocyte subsets

We further assessed the effect of STING-L administration on T and NK cell subsets. NK cell counts in the blood gradually decreased from 8 hpa of STING-L administration and returned to steady-state levels by day 7 in both groups (Figures 4A, 4B, S4A, and S4B). An assessment of T cell subsets showed that the proportion and number of CD4 or CD8 T naive, T central memory, and T effector memory/T effector cells (hereafter referred to as Tn, Tcm, and Tem/Teff, respectively) changed gradually upon STING-L administration before returning to normal within 3 days (Figures 4C, 4D, and S4C). The potentially adverse effect of STING-Ls on the T and NK cell subsets was transient but reversible; however, the recovery kinetics of these cells were faster than those of NK cells, consistent with a previous report showing that human NK cells are more susceptible to cell death than T cells.[38]

Next, the activation and proliferation of T and NK cells were examined in the respective subsets (Figures S4E–S4O). As the timing of the activation peak differed in each macaque, the fold-induction frequency of activation/proliferation markers at the peak time point was analyzed relative to pre-administration values. Overall, increased expression of CD69/CD25/Ki-67 was observed in all NK subsets of ligand-treated groups; however, significant differences were only observed with specific subsets and ligands (Figure S4F). Collectively, these results suggest that a single dose of STING-Ls can potentially

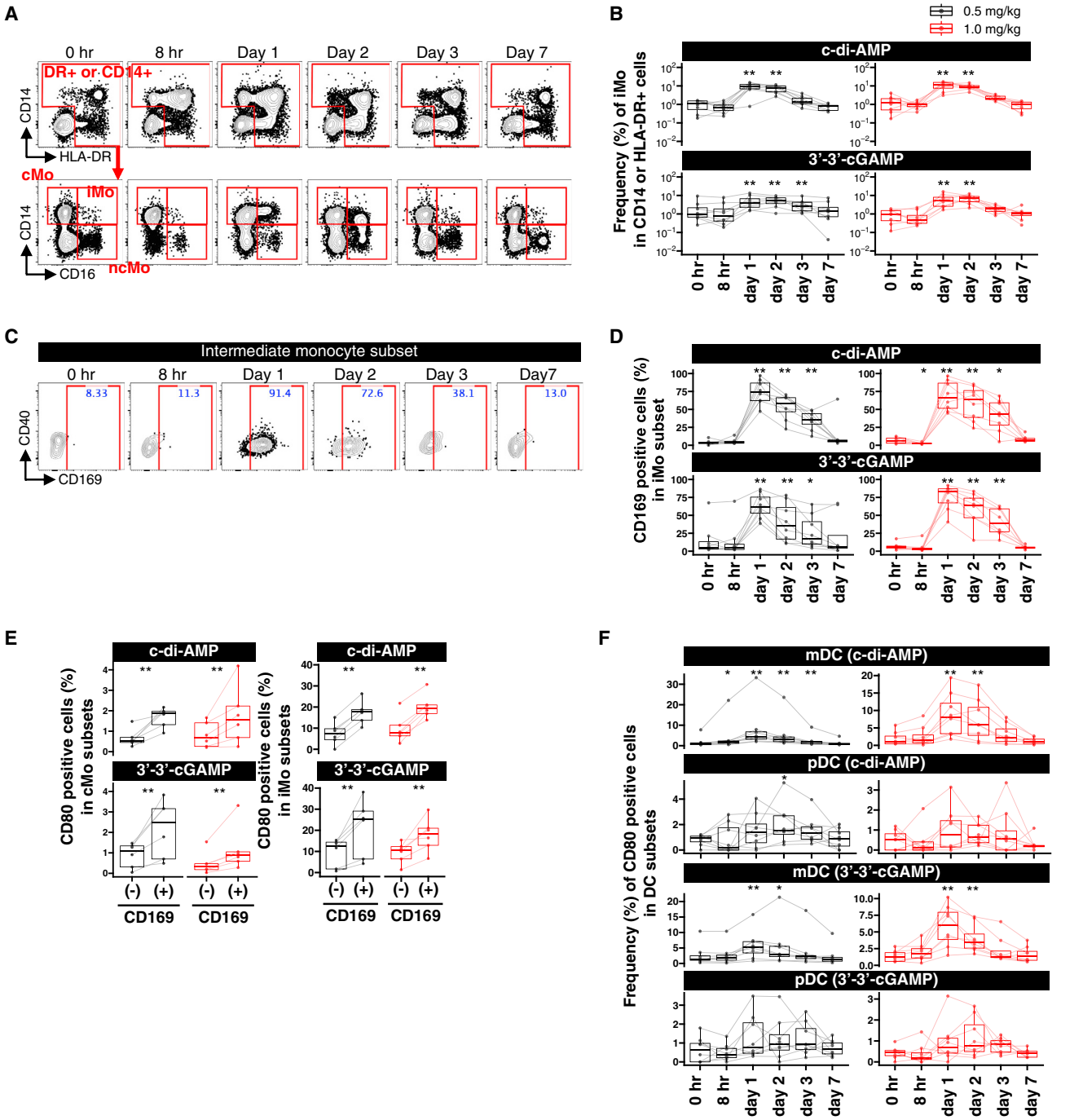

Figure 3. Effect of the administration of STING ligands on monocytes or dendritic cells (DCs)

(A) Representative flow cytometry data showing the kinetics of three distinct subsets within the total monocyte fraction analyzed based on CD14 and CD16 staining. cMo: classical monocyte, iMo: intermediate monocyte, ncMo: non-classical monocyte. Gating was performed based on CD14+ or HLA-DR+ cells in the CD3−CD20− population. (B) The kinetics of intermediate monocyte levels post-ligand administration are shown. (C) Representative flow cytometry data showing the kinetics of CD169-positive cells within the iMo subsets. (D) Graphs showing the kinetics of CD169 expression in the intermediate monocytes. (E) Graph for the frequency of CD80-positive cells in monocyte subsets at 1 day post-administration (dpa). Blue, black, and red dots/lines indicate the 0.1, 0.5, and 1.0 mg/kg dose, respectively. (F) The kinetics of CD80 expression in DC subsets are shown. Blue, black, and red dots and lines indicate the 0.1, 0.5, and 1.0 mg/kg doses, respectively. *p* values were calculated by Wilcoxon signed-rank test (0 hr vs each timepoint or negative vs positive). Statistical significance for (B) and (D)–(F) is indicated using * for the values $*p < 0.05$ and $**p < 0.01$.

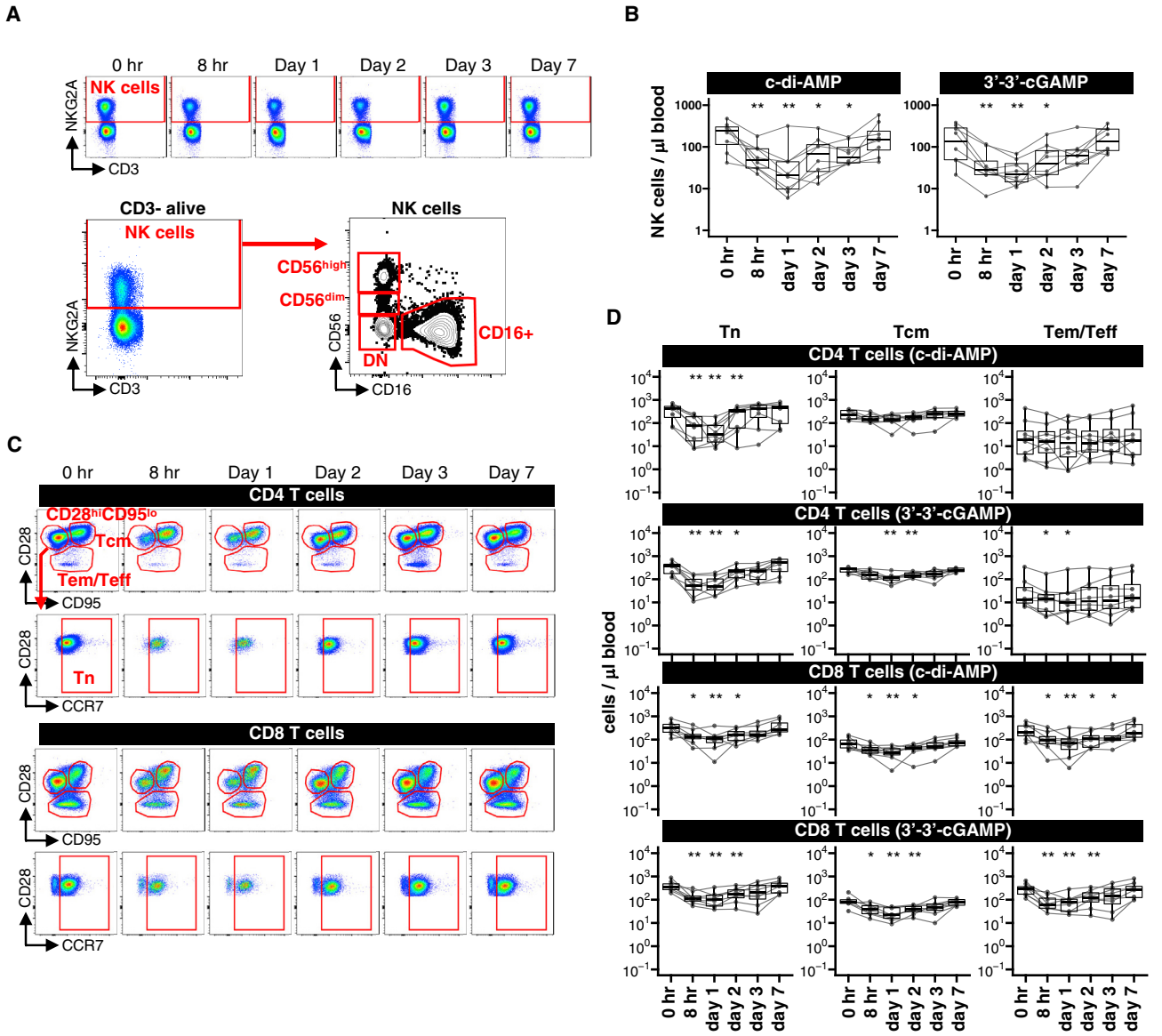

Figure 4. Effect of STING ligands on lymphocytes

(A) Representative flow cytometry data showing the change in the NK subset post-STING-L administration (top) and the NK subsets with CD56 and CD16 staining (bottom). DN: double-negative. (B) Graphs for the kinetics of NK subsets post-STING-L administration. (C) Representative flow cytometry data showing the change in CD4 T cell (top) or CD8 T cell (bottom) subsets post-STING-L administration. (D) Graphs for the kinetics of the number of T cell subsets in blood after 1.0 mg/kg STING-L administration. *p* values were calculated by Wilcoxon signed-rank test (0 hr vs each timepoint). Statistical significance is indicated using * for the values $*p < 0.05$ and $**p < 0.01$.

induce the transient activation of NK cells in the blood of cynomolgus macaques.

As observed for NK cells, CD69-positive cell counts in the Tcm and Teff/Tem groups increased within 3 days; however, significant differences were observed in the c-di-AMP-treated group alone (Figures S4H and S4J). Similarly, no significant changes in CD25, Ki-67, and PD-1 (a representative checkpoint molecule), as well as the chemokine receptor CXCR3 and transcription factor T-bet, both of which are functional markers of CD8 T cells, were noted (Figures S4H and S4J); however, no markers were commonly upregulated by STING-L administration, except PD-1 expression in CD8 Tem/Teff cells.

The systemic administration of STING-L has been reported to induce a tolerogenic response via mDC and Treg activation in a mouse model.[39] Therefore, we examined the frequency and activation of Tregs—FoxP3- and CD25-positive cells— in the CD4 T total memory subset (Figure S4D). The Treg frequency was reduced in the STING-L-treated

groups (Figure S4L), and Treg activation was observed in the c-di-AMP-treated group. The frequency of Ki-67-positive cells among Treg populations was significantly increased in both groups (Figure S4M), suggesting that STING-Ls potentially induce Treg proliferation.

To directly compare the activation status of each NK and T cell subset, NK and T cell activation data were summarized based on mean values and plotted as radar plots (Figure S4O). The induction of CD69 was most prominently observed in the $CD56^{dim}$ NK subset and Tem/Teff subsets of CD4 and CD8 T cells. Furthermore, c-di-AMP resulted in a higher mean value than 3′-3′-cGAMP, but no clear dose dependency was observed. Collectively, these results indicate that a single dose of STING-Ls transiently activates T and NK cells in cynomolgus macaques and that c-di-AMP is a better inducer of this activation. Of note, transient B cell activation was also observed; however, for simplicity and to focus on T and NK cells, we omitted the B cell data from the subsequent analysis (Figures S4P–S4S). Lastly, the fold-induction of CD69 in both CD4 and CD8 Tem/Teff cells was correlated with the levels of IFN-α at 1 dpa (Figures S4T and S4U), suggesting that the activation of T cells potentially depends on the induction of type I IFN.

Simultaneous evaluation of safety and efficacy by multi-parameter analysis

To evaluate the safety and efficacy responses in individual macaques, we performed principal component analysis (PCA) using the datasets reflecting the safety or efficacy aspect of the responses obtained before (T0: 0 hpa) and after (T1: peak, at which the maximum response was observed) administration. PC1 values from the PCA-safety (PC1-safety, Figure S5A, left) and PCA-efficacy (PC1-efficacy, Figure S5A, right) data were plotted to visualize the relationship between safety and efficacy (Figures 5A and S5B). The results showed clustering of the T0 and T1 subsets. The local responses in each macaque were re-analyzed to validate the results of the PCA. High occurrence values for erythema correlated with higher PC1-safety values, and the results partially reflected local erythema responses without using local parameters for plot generation (Figure S5C).

Next, to examine the magnitude of the response efficacy in individual macaques, we classified the macaques into two groups, good (R1 and R2 in Figure 5A) and poor efficacy (R3 in Figure 5A) groups, based on the PC1-efficacy values. Compared with that in the 3′-3′-cGAMP group, the c-the di-AMP group frequently showed a good profile (Figure 5B). Dose and ligand dependency was examined by PC1 safety or efficacy values. There were no dose-dependent differences (Figure 5C), and the 3′-3′-cGAMP group showed higher PC1-safety values (Figure 5D), suggesting that c-di-AMP is safer than 3′-3′-cGAMP. Though ligand-dependent differences in PC1 efficacy values were not observed, a higher fold-induction of CD69 in the c-di-AMP group compared with that in the 3′-3′-cGAMP group was observed (Figures 5E and 5F), suggesting that c-di-AMP is better in terms of efficacy as well. Taken together, we concluded that the i.m. administration of 0.5 mg/kg c-di-AMP would be the optimal condition to observe a better efficacy and safety profile.

Prediction of STING-L administration efficacy responses

We next determined if pre-administration immunological variables could predict the magnitude of the response efficacy to STING-L in individual macaques. We hypothesized that a key variable for response prediction would be the expression of the STING receptor. The *in vivo* effects of STING-L on various subsets of PBMCs, as summarized previously herein, indicate that these could serve as direct ligand targets. STING is expressed ubiquitously[6–8]; however, steady-state STING expression in each PBMC subset is not well characterized. Therefore, we investigated STING expression in each PBMC subset using multicolor flow cytometry. Using an anti-STING antibody clone validated with a STING-KO line (Figure S6A), we examined STING expression in cynomolgus macaque PBMCs. Antibody-specific signals were detected in all subsets analyzed (Figures 6A and S6B–S6D), although the difference between the isotype control and STING antibody staining was not obvious in B cells, several NK subsets, and neutrophils. STING expression was observed in DCs, monocytes, T cells, and $CD56^{high}$ NK cell subsets. Next, we compared the frequency of STING-positive cells in each subset. Monocytes showed the highest percentage of STING-positive cells, and CD4 T cells showed a higher percentage of STING-positive cells than CD8 T cells among the T cell subsets (Figures 6B and 6C). STING expression levels were different in each macaque, but macaques showing greater STING expression in one subset tended to have higher STING levels in other subsets, indicating that expression is regulated in individual macaques at the whole PBMC level. Correlation analysis revealed that most of the parameters indicating STING expression were highly correlated with each other (Figure S6E); however, those did not correlate with cytokine expression. There was even a slight inverse correlation between the percent STING+ cells among pDCs and the levels of IFN-α at 8 hpa (Figure S6F left), but not at 1 dpa, suggesting that type I interferon induction is unlikely to depend on STING expression levels. Similarly, a correlation between STING expression and the levels of IL-1RA at 1 dpa, but not at 8 hpa, was observed (Figure S6F right). These data suggested that the level of cytokine production may not depend on the level of STING expression.

To predict the magnitude of the response efficacy, we selected parameters that contributed to the differences between good- or poor-efficacy groups using standard statistical tests (Figure 6D). Among the 55 parameters analyzed in each dataset, twenty-six showed significant differences (Figure S7A). The heatmap and boxplots revealed clear differences between the two groups (Figures 6E and S7B). Based on the selected parameters, the macaque responses were further characterized using additional PCA. Interestingly, groups with good or poor efficacy were partially clustered based on the pre-administration variables obtained from the blood analysis (Figure 6F), suggesting that these parameters could be useful as biomarkers to predict responses before STING-L administration. To validate the prediction of good and poor profiles, the leave-one-out cross-validation approach was applied using three methods (Figure S7C). The data demonstrated that either the neural network- or random forest-based method resulted in more than 70% accuracy (Figure 6G).

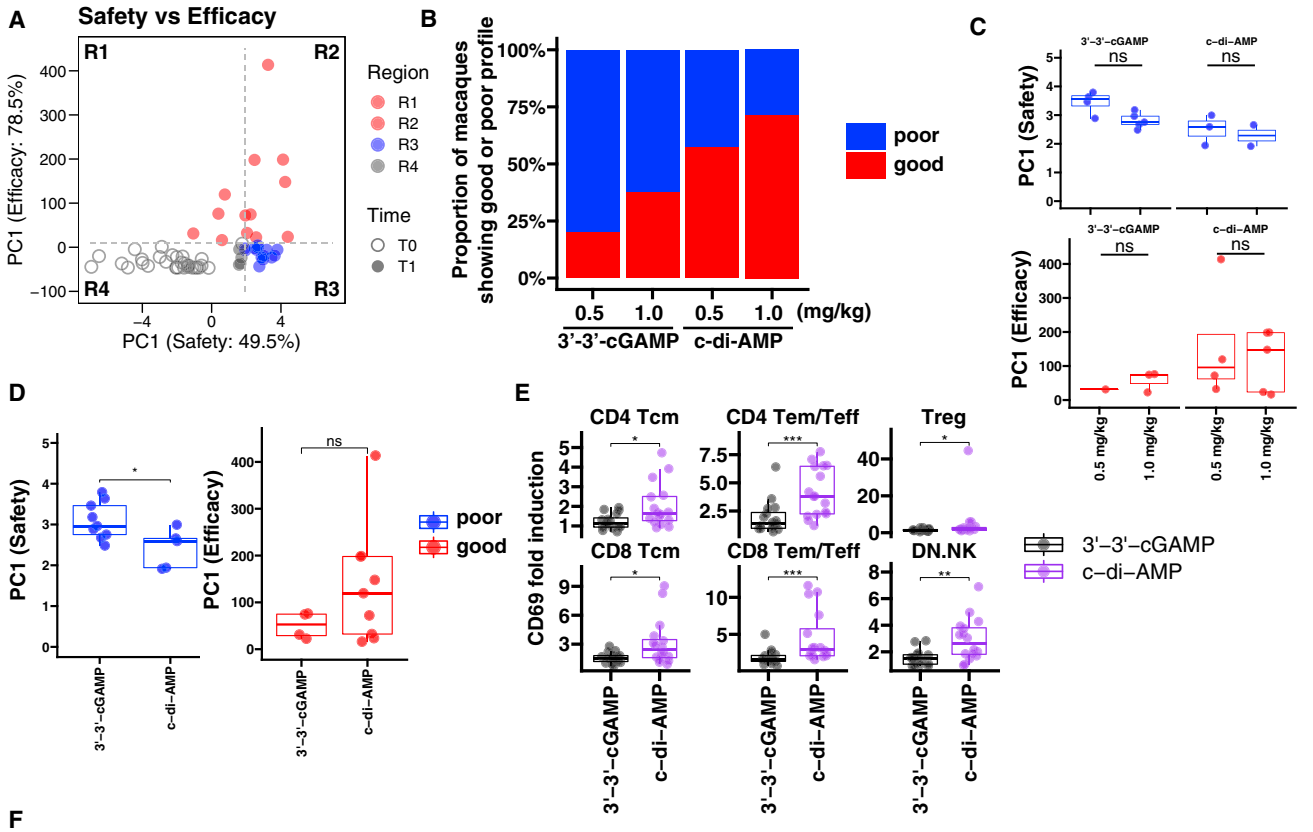

F

Characteristic	Overall N = 32[1]	3'-3'-cGAMP N = 16[1]	c-di-AMP N = 16[1]	p-value[2]
FACS: CD69 fold induction in CD8Tem/Teff	2.11 (1.57, 3.17)	1.57 (1.35, 2.14)	2.99 (2.11, 5.75)	<0.001
FACS: CD69 fold induction in CD4Tem/Teff	2.26 (1.34, 3.91)	1.43 (0.97, 2.37)	3.81 (2.24, 6.47)	<0.001
FACS: CD69 fold induction in CD16+NK	1.79 (1.35, 2.88)	1.52 (1.07, 1.78)	2.60 (1.81, 3.81)	0.002
FACS: PD-1 fold induction in CD4Tem/Teff	1.16 (1.00, 1.47)	1.04 (0.92, 1.26)	1.35 (1.12, 1.68)	0.003
FACS: Ki-67 fold induction in CD4Tcm	1.19 (0.98, 1.45)	1.37 (1.20, 1.49)	0.98 (0.74, 1.14)	0.008
ELISA: IFNa	63 (27, 86)	43 (14, 65)	81 (38, 99)	0.012
FACS: CD69 fold induction in CD4Treg	1.66 (1.26, 2.23)	1.34 (1.14, 1.69)	1.89 (1.64, 2.80)	0.015
FACS: CD69 fold induction in CD4Tcm	1.32 (1.05, 1.81)	1.15 (0.94, 1.41)	1.63 (1.27, 2.50)	0.017
FACS: CD69 fold induction in CD8Tcm	1.72 (1.35, 2.72)	1.54 (1.20, 1.81)	2.41 (1.60, 3.47)	0.017
FACS: Ki-67 fold induction in CD8Tcm	1.59 (1.06, 1.91)	1.75 (1.58, 1.97)	1.14 (0.91, 1.61)	0.021
FACS: % intermediate monocytes	7.1 (3.4, 11.5)	4.4 (2.5, 8.0)	10.0 (6.9, 14.8)	0.021
FACS: Ki-67 fold induction in DN.NK	1.47 (1.05, 2.03)	1.85 (1.32, 2.31)	1.17 (0.96, 1.62)	0.039
FACS: PD-1 fold induction in CD4Treg	1.51 (1.30, 2.16)	1.38 (1.25, 1.50)	1.96 (1.51, 2.48)	0.047

[1]Median (IQR); n (%)

[2]Wilcoxon rank sum test; Wilcoxon rank sum exact test; Fisher's exact test

Figure 5. Multi-parameter analysis of the effect of STING ligands

(A) Scatterplot depicting the PC1 values from two principal component analyses (PCAs) for safety and efficacy. Filled circles indicate the time points (T0: pre, T1: post). The colors indicate regions gated using the highest values of T0. (B) Proportions of macaques showing good or poor profiles are shown. (C) The PC1-safety (top) or PC1-efficacy (bottom) in each dose group is shown. The colors indicate the efficacy groups defined by PC1 (efficacy; Good: good efficacy profile; Poor: poor efficacy profile). (D) PC1-safety (left) or PC1-efficacy (right) in each ligand group is shown. (E) CD69 induction in each ligand group is shown. (F) The statistically significant parameters and results of statistical tests comparing two STING ligands are shown as a table. Red text indicates higher values. *p* values were calculated by Mann-Whitney U test. Statistical significance is indicated using * for the values $*p < 0.05$, $**p < 0.01$ and $***p < 0.001$.

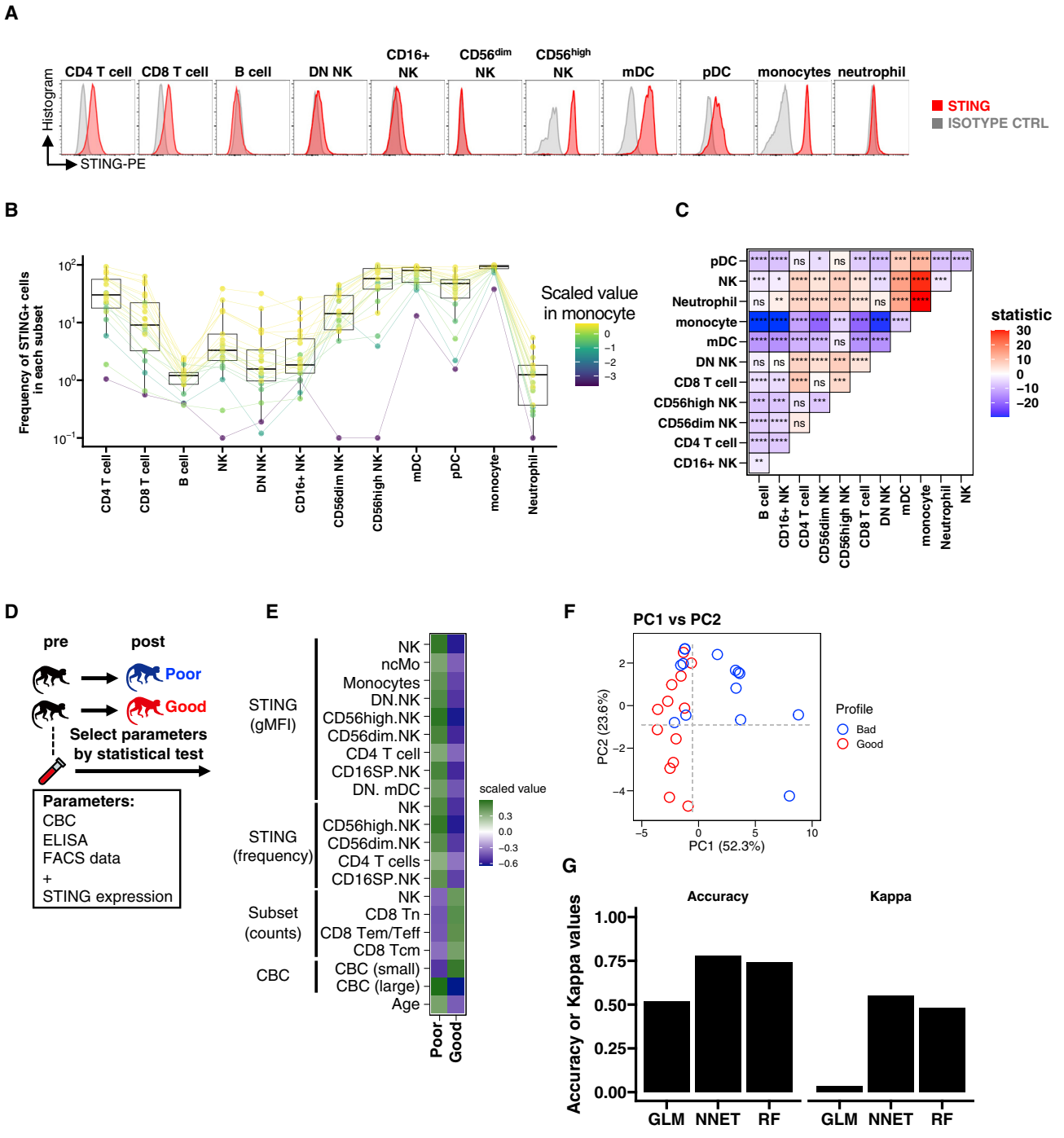

Figure 6. Prediction of the effect of STING ligands using multi-parameter analysis

(A) Representative flow cytometry data for anti-STING-PE (red) or isotype-PE (gray) staining in each peripheral blood mononuclear cell (PBMC) subset. (B) Boxplots for frequency of STING-expressing cells in each subset. The values are background (isotype-PE) subtracted. Colors indicate the scaled value in monocytes. (C) The result of statistical comparison of STING expression between each subset is shown as a heatmap. Statistical significances calculated by Wilcoxon signed- rank test are indicated using asterisks (as adjusted *p* values for multiple comparisons). To show which subset is higher in each comparison, colors indicate the statistic value from paired Student's t test; blue indicates higher in the subset shown on y axis; red indicates higher in the subset shown on x axis. (D) Schematic depiction of the prediction of poor or good profiles. (E) Heatmap of the mean value at T0 for each parameter in the two groups (Good: good efficacy profile; Poor: poor efficacy). Original values were scaled, and variances were

(legend continued on next page)

Aging is associated with blunted type I IFN responses

Among the parameters contributing to the prediction of a good or poor profile, age was identified as one of the top-ranked parameters (Figure S7C). Increasing age affects the immune system's properties and capacity, a process often referred to as immunosenescence.[40] We, therefore, investigated the effect of aging on the response to STING-L in more detail. Although animal age distribution was equal among experimental groups in our study design (Figure S8A), it was higher in the poor-efficacy group (Figure 7A), in which the production of functional cytokines was lower (Figure 7B). Further, lymphocyte and neutrophil numbers at pre-administration were inversely and positively correlated, respectively, with age (Figure 7C), consistent with our previous findings using human PBMCs, where the balance between lymphoid precursors and myeloid precursors was shifted toward myeloid precursors with aging due to altered hematopoiesis of hematopoietic progenitor cells.[41] Inverse correlations between age and functional cytokine production (Figure 7D) suggest that age is associated with efficacy outcomes. In addition, erythema-related parameters were correlated with age (Figure 7E), suggesting that age is also associated with local inflammatory responses induced by STING-L. Interestingly, pDC activation was inversely correlated with age (Figures 7F and S8B), suggesting that the age-dependent reduction in pDC activation would be one of the reasons for the blunted type I IFN responses in older monkeys. Lastly, to validate the effect of aging on the production of cytokines induced by the *in vivo* administration of STING-L, we utilized an additional aging cohort. In this cohort, monkeys were categorized into young and older groups (Figure 7G left), and naive T cells were reduced in the older group (Figure 7G right). *In vitro* stimulation of PBMCs by STING-L induced IFN-γ production in both groups; however, older monkeys had lower IFN-γ levels than young ones (Figure 7H), although the level of IFN-α and IL-6 was not different between the age groups (data not shown).

DISCUSSION

The selection of the ligands, their dose, and their administration route are critical for eliciting beneficial immune activation with immunomodulatory drugs. Here, we investigated the safety and efficacy of two clinical grades of STING-L *in vivo* in NHPs. Using dose-escalation experiments via two routes, we demonstrated systemic inflammatory responses for doses up to 1.0 mg/kg, including a change in CBCs and the transient increase and activation of iMos. Concurrently, the number of T and NK cells in the blood decreased immediately after STING-L administration but recovered within 3–7 days. The local edema and erythema responses resolved within 2 weeks, indicating that a single i.m. administration of these ligands was safe up to a dose of 1.0 mg/kg.

Recently, the effects of two novel STING-Ls, ADU-S100 and CF501, in rhesus macaques were reported, the first for suppressing nociception[33] and the second as an adjuvant for the COVID-19 vaccine.[34] However, neither study assessed the safety of ligand administration in detail. Therefore, this study is the first to demonstrate the safety of STING-L using NHP models.

Tumorigenesis can be suppressed immunologically; however, tumor immunogenicity can be altered to increase host immunocompetence. This concept is termed "cancer immunoediting" and originated from the immunosurveillance hypothesis.[42] The induction of type I IFN and IFNγ is independently associated with immunosurveillance, and the cross-priming of tumor-specific CD8 T cells is key for tumor suppression.[43,44] In addition to tumorigenesis suppression, type I IFNs contribute to tumor regression in various anticancer therapies, including radiation and the activity of antibodies against growth factors, immunomodulatory drugs, oncolytic viruses, and checkpoint inhibitors.[45]

STING activation by tumor-derived cytosolic DNA, or the administration of STING-L, and the consequent production of type I IFN primes tumor-specific CTLs.[20,46,47] To evaluate the efficacy of STING-L, we examined the functional cytokines induced in the plasma. Consistent with the results of a previous *in vitro* study,[4] IFN-α and IFN-γ levels were upregulated in response to c-di-AMP and 3'-3'-cGAMP administered at high doses (>0.5 mg/kg). Furthermore, the transient activation of DCs was found to have the same kinetics as those of cytokines, indicating that both ligands can potentially enhance the activity of T/NK cells by conditioning the environment for lymphocytes via DC activation.

STING is expressed in multiple cell types, and cell-type-specific intrinsic STING activity has been demonstrated. To evaluate the consequences of STING-L administration, the effect on different cell types should be examined carefully. A recent *in vitro* study showed that CD169-expressing monocytes boost the capacity for the cross-presentation of antigens to CD8 T cells in human PBMCs.[37] Therefore, the upregulation of CD169 levels induced by STING-L in monocytes could enhance T cell immunity. Consistently, expression of the CD80 co-stimulatory molecule in monocyte subsets was upregulated in CD169-positive subsets, as shown in human PBMCs.

Among DC subsets, mDCs are known as professional antigen-presenting cells, and pDCs are considered the source of type I IFN production.[48] Therefore, type I IFN production by mDCs is generally underestimated. In our study, the transient activation of mDCs was observed in the ligand-treated macaques, although pDC activation was only observed in some macaques (Figure 3F). Results from an *in vitro* study showed that STING-L triggers type I IFN production in human pDCs, with increased expression of co-stimulatory molecules.[49] *In vivo*, mDCs, but not pDCs, were shown to be the source of type I IFN after infection

adjusted to 1. Maximum and minimum values were colored green or violet. (F) Principal component analysis (PCA) plot generated using selected parameters at T0 based on the statistically significant data shown in Figure S5D. The colors indicate the efficacy groups defined by PC1 (efficacy; Good: good efficacy; Poor: poor efficacy). (G) Graphs show the accuracy or kappa values of prediction cross-validated by the leave-one-out cross-validation method. The x axis indicates the method used to predict good or poor profiles by machine learning (three distinct modeling algorithms were used; GLM, generalized linear models; NNET, neural network classifier; RF, random forest model).

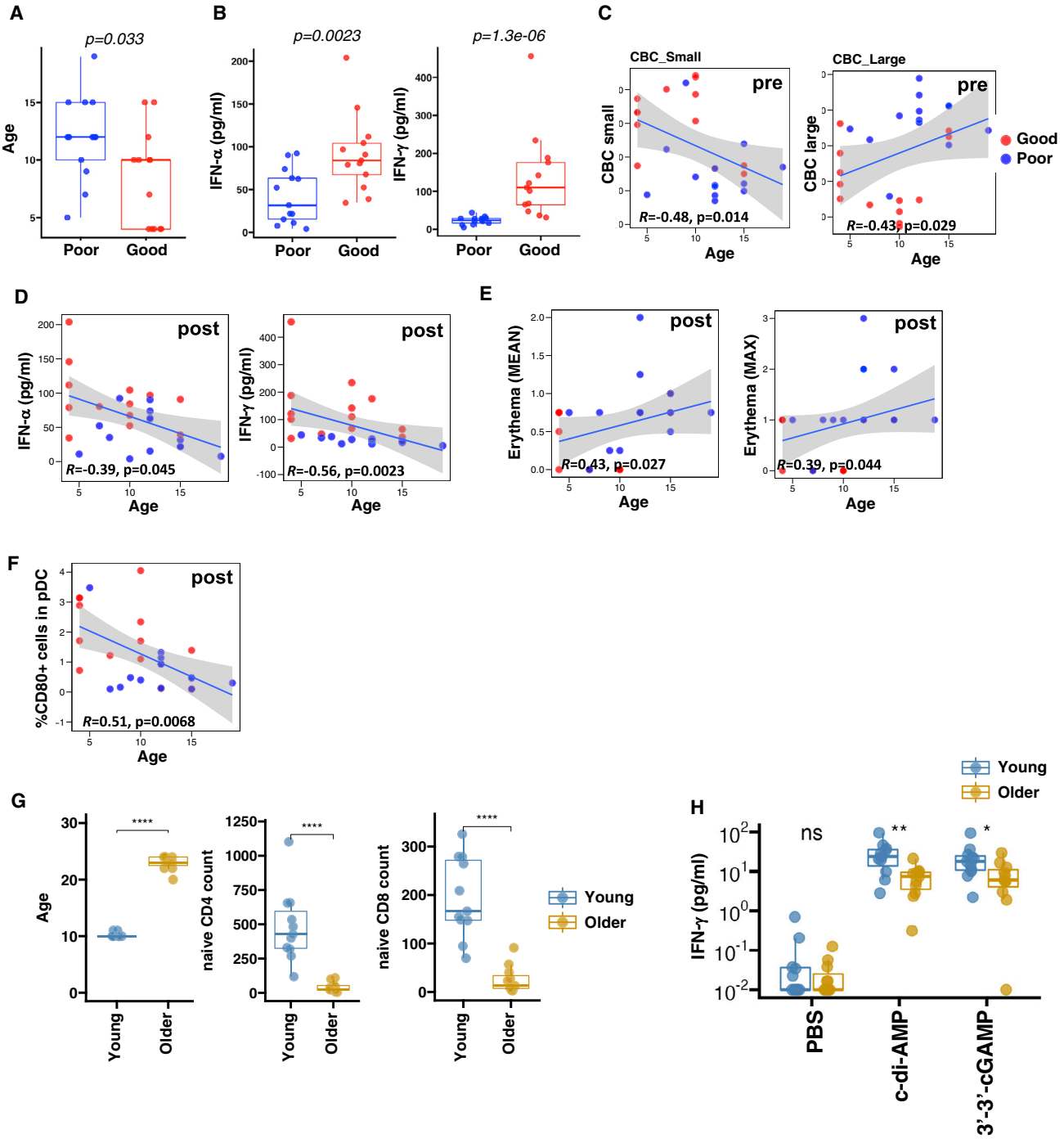

Figure 7. Age-dependent changes in responses induced by STING ligands

(A) Boxplots showing the age in the Good vs. Poor profile groups. (C) Scatterplot showing the correlation between age and lymphocytes (CBC_small, left) or neutrophils (CBC_large, right) before STING ligand administration, as determined by complete blood counts (CBCs). (D) Scatterplot showing the correlation between age and IFN-α (left) or IFN-γ (right) at 1 dpa. (E) Scatterplot showing the correlation between age and statistical values of local inflammation; MEAN (left) or MAX (right). (F) Scatterplot showing the correlation between age and immunological values; percent CD80$^+$ among plasmacytoid dendritic cells (pDCs). (G) Boxplots showing the age (left) and naive T cell count (middle and right) in young vs. older groups derived from macaques of another cohort. (H) Boxplots showing IFN-γ expression in young vs. older groups after *in vitro* STING stimulation. *p* values were calculated by Mann-Whitney U test (A, B, G, H) or Spearman's correlation analysis (C, D, E, F). Statistical significance is indicated using * for the values $^*p < 0.05$, $^{**}p < 0.01$ and $^{****}p < 0.0001$.

with TLR-independent viruses and subsequent STING activation.[50] Taken together, both DC subsets could be a source of type I IFN and contribute to the antitumor effects mediated by STING-L.

NK cells are cytotoxic lymphocytes and are especially important for controlling poorly immunogenic tumors.[51] A recent study showed that the NK cell-dependent killing of tumor cells *in vivo* requires the enzymatic activity of cGAS to produce tumor-derived cGAMP, which in turn activates STING in host cells.[52] In this study, we analyzed the activation of each NK subset via CD69 expression analysis, and the results indicated that ligand-dependent NK activation is commonly observed independent of CD16 and CD56 expression. In contrast, tumor proliferative activity, analyzed based on Ki-67 expression levels, was observed when 3'-3'-cGAMP was used. A similar 3'-3'-cGAMP dependency was also observed in CD4 and CD8 T cells. CDN-dependent differences in effector functions are well documented in bacteria,[13] although the differences in mammals remain unclear. One explanation for the ligand-dependent exertion of downstream functions relates to the steric effect during binding to STING,[19] as human STING showed a reduced IFN response to 3'-3'-cGAMP compared with 2'-3'-cGAMP. Alternately, unidentified oligodeoxynucleotide partners may be associated with the effect differences observed. For instance, the oxidoreductase RECON binds to the bacterial CDNs, but not eukaryotic CDNs, and antagonizes the STING pathway.[53]

Recently, $PD1^{high}$ $TCF1^{+}$ CD8 T memory stem (Tscm) cells have been shown to play a pivotal role in controlling tumors.[21,22] STING-L increases the Tscm frequency when naive CD8 T cells are treated *in vitro*, and STING-L administration *in vivo* activates the antitumor response owing to an increase in CD8 Tscm cells.[54] Consistent with these results, STING-L induced an increase in the number of CD69-positive activated CD8 T cells, and PD-1 expression was increased in CD8 Tem/Teff cells.

STING is expressed in human PBMCs, DCs, monocytes, and T cells but not in macrophages and B cells.[29,55] Thus, the administration of STING-L can potentially induce a wide range of cellular responses in various cell types. In addition to type I IFN production, the modulation of intrinsic T cell activity by STING-L has recently been demonstrated in CD8 T cells.[54] Thus, prior knowledge of cell types that are potentially affected by the administration of STING-L is important for developing STING-L as a therapeutic agent. We examined STING expression in the main cell subsets of cynomolgus macaque PBMCs using multicolor flow cytometry. As in human PBMCs, higher expression of STING was observed in monocyte and DC subsets in cynomolgus macaques. Additionally, NK, CD4, and CD8 T cells were present at lower levels than monocytes/DCs, consistent with proportions in human PBMCs.[29,55] STING expression in neutrophils and B cells was low, but distinct STING-positive cells were observed, suggesting that these cells can potentially express STING under certain conditions. Consistent with these results, STING expression in B cells has been reported in mice.[56] Further analysis is required to clarify the expression of these subsets.

Variables derived from individual genetic, physiological, and pathological backgrounds are hurdles to the success of clinical trials. To overcome these limitations, a systems biology approach for vaccine development, called "systems vaccinology," has emerged as a new concept to analyze vaccine outcomes.[57] Using systemic multi-parameter analysis, the efficacy of the influenza vaccine was predicted before vaccination.[58] Compared with the uniform genetic background of mice, NHPs have several genetic backgrounds within species, which potentially reflects the diverse responses in humans. Therefore, we investigated the individual differences induced by STING-L. In our model, complex phenotypes associated with safety and efficacy described by the multiple experimental data were converted to simple values using a dimensional deduction approach, and a better safety and efficacy profile was demonstrated in the c-di-AMP group compared with that in the 3′-3′-cGAMP group.

Age emerged as a key determinant of the grouping of good or poor profiles, illustrating the effect of aging and immunosensecence[40] on *in vivo* responsiveness to STING-L. Age was higher in the poor profile group and correlated with the level of functional cytokines. Given the inverse correlation between pDC activation and age, we hypothesized that an age-dependent decrease in pDC activation could contribute to the diminished type I IFN induction in older individuals. Though we could not find a correlation between the level of proinflammatory cytokines and age (data not shown), the local inflammatory response was positively correlated with age, suggesting that aging affects not only the efficacy but also the safety of immunomodulatory drugs. These age-related safety and efficacy profiles of STING-L align with previous findings with other ligands for PRRs in human PBMCs.[59] Our work provides the first *in vivo* demonstration of such effects in primates to our knowledge.

This study has several limitations. In this study, we analyzed immune parameters mostly from cells in the blood but not at the injection site, where the STING-L concentration is likely to be the highest. As pDC is known to be activated in tissues,[60,61] the immune profiling of tissues would give a different perspective. In this study, we did not show vehicle-only treatment controls due to the limitation of available monkeys. Nevertheless, we previously showed that type I IFNs was not upregulated by vehicle-only treatment in a study of TLR9 agonists on macaques from the same colony.[35] Further, we confirmed the expression of STING only at the base level and did not analyze the variation in response to positive feedback from type I IFN. Additionally, the expression levels of various key signaling molecules downstream of the cGAS–STING pathway were not evaluated. Lastly, cytokine measurements in this study were performed by ordinary ELISA and not by highly sensitive ELISAs such as SIMOA. We believe that the accuracy of prediction may be further improved by addressing these limitations. Besides, the study was also limited due to the number of monkeys available, and the selection of individuals to allow averaging the sex and weight differences was not possible. Nevertheless, in the macaques used in this study, we did not observe any effect of weight or sex on the outcome of STING-L administration (data not shown).

To conclude, based on a refined examination of local or systemic inflammation, the activation and STING expression on the main immunocompetent cell subsets in cynomolgus monkeys, we propose that 0.5 mg/kg c-di-AMP i.m. administration is the optimal starting point for clinical studies. This efficacy outcome was partially predicted based on physiological or immunological parameters obtained before ligand administration. This study contributes to the development of future STING-L-based immunomodulatory therapies/vaccines for cancer or infectious disease, and the methodology described herein could apply to the development of other therapeutic agents in preclinical stages.

MATERIALS AND METHODS

Animal experiments, PBMC sampling, and hematological analysis

Cynomolgus macaques, negative for SIV, simian type D retrovirus, simian T cell lymphotropic virus, simian foamy virus, Epstein-Barr virus, cytomegalovirus, and B virus, housed at the Tsukuba Primate Research Center (TPRC), the National Institutes of Biomedical Innovation, Health, and Nutrition (NIBIOHN), were used in this study. In total, 44 cynomolgus macaques with ages ranging from 4 to 20 years were divided into three groups for either ligands: 0.1 mg/kg dose (n = 6), 0.5 mg/kg (n = 8), and 1.0 mg/kg (n = 8) (Table S1). Animals of different ages were adjusted between groups (Figure S8A). Macaques were administered an increasing dose of either c-di-AMP or 3'-3'-cGAMP intramuscularly at 1-month intervals. Animal studies were performed at NIBIOHN with approval from the Committee on the Ethics of Animal Experiments of NIBIOHN (Approved #DSR03-22). The animals were supervised by the veterinarians in charge of the animal facility. PBMCs and plasma were isolated from blood samples collected at each time point into tubes containing EDTA using Ficoll-Paque PLUS (GE Healthcare, Buckinghamshire, UK). Purified PBMCs were incubated in fetal bovine serum (Sigma-Aldrich, St. Louis, MO, USA, hereafter Sigma) containing 10% DMSO (Sigma, St. Louis, MO, USA) and stored in liquid nitrogen until analysis. CBCs were performed using freshly isolated blood with an automated hematology analyzer (Sysmex K-4500; Sysmex, Hyogo, Japan).

Scoring of the local inflammatory response

Local symptoms at the administration site were visually examined by a veterinarian, and scoring was performed before dose administration and at 0 h, 8 h, 1dpa, and subsequently every day for 14 days. The grades were defined according to a previously described method,[62] and the detailed criteria are listed in Table S2. Briefly, a total of five grades were used, including 0 (none), 1 (minimal), 2 (mild), 3 (moderate), and 4 (severe). To evaluate the overall responses of the individual macaques, statistical parameters, including the mean (mean score per day), max (maximum score within 14 days), and occurrence (total number of time points at which a score greater than 1 was detected), were calculated.

ELISA or Bio-Plex assay

Plasma was obtained from the blood supernatant during PBMC purification and was cryopreserved until further use. Plasma cytokine levels were analyzed using ELISA kits purchased from MABTECH (Nacka Strand, Sweden) for evaluating monkey IL-6 (3460-1H-6), monkey IFN (3421M-1H-6), human IFN (3425-1H-6), and human IL-12/23 p40 (3450-1H-6). IL-1RA levels were analyzed using the ProcartaPlex NHP immunoassay (IL-1RA, eBioscience) according to the manufacturer's protocol. ELISA signals were detected using a Luminex 200 device (Luminex).

Flow cytometric analysis

Frozen PBMCs were thawed and washed with Roswell Park Memorial Institute 1640 medium (Sigma), supplemented with 10% FBS (Sigma), 100 unit/mL penicillin, and 100 mg/mL streptomycin (Sigma, the supplemented medium hereafter, R10). The cells were treated with 1 mL of 50 U/mL benzonase (Merck, Darmstadt, Germany) in R10 for 30 min at 37°C. After incubation, the cells were stained using the Fixable Viability Stain 440UV kit (FVS440, Becton, Dickinson, and Co., Franklin Lakes, NJ, USA; hereafter BD) at room temperature (hereafter RT) for 5 min. The cells were subsequently seeded into two plates. Half the cells were stained using a monocyte/DC panel (Table S3), whereas the other half of the cells were stained with the T/NK panel (Table S4). The CC-chemokine receptor 7 (CCR7) was stained at 37°C for 10 min, and the antibodies for the remaining markers listed in the Tables S3–S4 were added and incubated at RT for 15 min. Next, intracellular staining was performed with the Transcription Factor Buffer Set (BD) according to the manufacturer's protocol. After staining, cells were washed twice with PBS, fixed with 1% paraformaldehyde, and analyzed using the FACSymphony A5 flow cytometer (BD) equipped with 5 lasers. For intracellular STING analysis, cells stained with FVS440 were blocked with an FcR blocking reagent (Miltenyi Biotec, Bergisch Gladbach, Germany) for 10 min at RT. Next, cells were stained with surface antibodies listed in Table S5 for 15 min at RT. After washing twice with PBS, cells were fixed with Lyse/Fix buffer (BD) at 37°C for 10 min, followed by centrifugation to remove the Lyse/Fix buffer, and were permeabilized with Cytofix/Cytoperm (BD) at RT for 10 min. Cells were washed twice with Perm/Wash (BD) and stained with either STING-PE (clone: T3-680) or isotype-PE (clone: MOPC-21) for 20 min at RT. After washing twice, the cells were resuspended in 1% paraformaldehyde/PBS and were analyzed using the FACSymphony A5 flow cytometer.

Flow cytometry data processing for safety and efficacy evaluation of individual macaques

Flow cytometry FCS files were analyzed using the FlowJo software (version 10.8.1; BD). Plots were generated using the R software version 4.1.0. using the packages listed in Table S6. Absolute counts for NK and T cell subsets were calculated using the number of WBCs, the frequency of lymphocytes in WBCs, and the frequency of each subset in the lymphocyte gate.

Multi-parameter analysis for safety and efficacy evaluation of individual macaques

PCA was performed using the *prcomp* function in the R statistics package. PCA plots for safety and efficacy were generated separately using selected parameters (for safety, 16 parameters including CBC at 8 hpa, proinflammatory cytokine levels, the frequency and activation of iMo, and NK cells and T cell subset absolute numbers were used;

for efficacy, 33 parameters including functional cytokine levels and activation of DC, NK, and T cell subsets were used). Values were selected from two time points: the first from day 0 (T0), and the second (T1) from the maximum response post-administration (at 8 hpa for CBC or at 1 dpa for other parameters except for peak values, for which the original values were selected within 3 dpa). To create a plot that simultaneously showed analysis for safety and efficacy, PC1 values from the safety and efficacy PCA data were combined and plotted in two-dimensional space. Individual macaques were classified into two groups (good-efficacy [n = 16] and poor-efficacy groups [n = 16]) based on the PC1 values from the PCA-efficacy data to select the parameters that contributed to efficacy. The differences in 55 parameters at T0, including age and STING expression of each subset, were evaluated to compare the two groups using the Wilcoxon test, and 26 statistically significant parameters were obtained. The selected 26 parameters were used for a second PCA to predict the efficacy outcome. The parameter values for each macaque were scaled, and variances were set to 1 within each parameter by the *scale* function of the R scales package, and the mean values were plotted to create a heatmap using the ggplot2 package. Validation of the prediction was done by the leave-one-out cross-validation (LOOCV) approach by using three well-established machine learning (ML) algorithms (e.g., generalized linear models: GLM, random forests: RF, neural network: NNET). LOOCV is a cross-validation in which each individual split of the k-split cross-validation uses only one piece of data for testing and all the rest as training data. The ML modeling was performed using the *caret* package.

Measurement of *in vitro* cytokines

In vitro assessment of the ligand responses was performed as previously described.[4] Briefly, PBMCs obtained from young and older macaques were stimulated with 10 μg/mL c-di-AMP in R10 for 24 h. The cytokines accumulated in the culture supernatant were harvested and analyzed by ELISA, as described above.

Statistical analysis

Statistical analyses were performed using R/Bioconductor (R version 4.1.0) or GraphPad Prism (Version 8.3.0; GraphPad Software, San Diego, CA, USA). The experimental variables were compared using the nonparametric Wilcoxon signed-rank test or Mann-Whitney U test unless otherwise mentioned. The Kruskal-Wallis test was used for Figure 1C. Statistical significance was set at $p < 0.05$. For the cytokine correlation data, each value of cytokine concentration in plasma was scaled, and variances were adjusted to 1 within parameters by the *scale* function of the R scales package, and Spearman's correlation values were calculated.

DATA AVAILABILITY STATEMENT

Data are available from the corresponding author upon reasonable request.

SUPPLEMENTAL INFORMATION

Supplemental information can be found online at https://doi.org/10.1016/j.omtm.2022.12.008.

ACKNOWLEDGMENTS

This study was supported by the Japan Society for the Promotion of Science Grant-in-Aid for Scientific Research (B) (grant number 20H03728), Scientific Research (C) (grant number JP20K06405), and the Japan Agency for Medical Research and Development (grant numbers: 21fk0210057h0003, 21fk0410040h0001, 21nf0101627s0202, and 21wm0325015s0202). We would like to acknowledge Dr. Tomotaka Okamura at the Tsukuba Primate Research Center, National Institutes of Biomedical Innovation, Health and Nutrition, for valuable discussion and support. We also thank the members of the Laboratory of Immunosenescence, especially Eiko Moriishi, Mami Ikeda, Mika Yagoto, and Yuki Katayama, for their excellent technical support. We also thank HAMRI Co., Ltd. and the Corporation for Production and Research of Laboratory Primates for their support with animal experiments.

AUTHOR CONTRIBUTIONS

S.T. and T.Y. designed the research study. K.I. prepared the STING ligands. S.T. and T.N. performed experiments. S.T. performed the experiments and the multi-parameter and statistical analyses. S.T., V.A., and T.Y. wrote the manuscript. All authors have read and approved the manuscript.

DECLARATION OF INTERESTS

K.I. is an employee of Yamasa Corporation, Chiba, Japan. STING ligands used in this study were provided by the Yamasa Corporation.

REFERENCES

1. Kawai, T., and Akira, S. (2010). The role of pattern-recognition receptors in innate immunity: update on Toll-like receptors. Nat. Immunol. *11*, 373–384. https://doi.org/10.1038/ni.1863.

2. Rameshbabu, S., Labadie, B.W., Argulian, A., and Patnaik, A. (2021). Targeting innate immunity in cancer therapy. Vaccines *9*, 138. https://doi.org/10.3390/vaccines9020138.

3. Takahama, S., and Yamamoto, T. (2020). Pattern recognition receptor ligands as an emerging therapeutic agent for latent HIV-1 infection. Front. Cell. Infect. Microbiol. *10*, 216. https://doi.org/10.3389/fcimb.2020.00216.

4. Yamamoto, T., Kanuma, T., Takahama, S., Okamura, T., Moriishi, E., Ishii, K.J., Terahara, K., and Yasutomi, Y. (2019). STING agonists activate latently infected cells and enhance SIV-specific responses ex vivo in naturally SIV controlled cynomolgus macaques. Sci. Rep. *9*, 5917. https://doi.org/10.1038/s41598-019-42253-3.

5. Burdette, D.L., Monroe, K.M., Sotelo-Troha, K., Iwig, J.S., Eckert, B., Hyodo, M., Hayakawa, Y., and Vance, R.E. (2011). STING is a direct innate immune sensor of cyclic di-GMP. Nature *478*, 515–518. https://doi.org/10.1038/nature10429.

6. Ishikawa, H., and Barber, G.N. (2008). STING is an endoplasmic reticulum adaptor that facilitates innate immune signalling. Nature *455*, 674–678. https://doi.org/10.1038/nature07317.

7. Sun, W., Li, Y., Chen, L., Chen, H., You, F., Zhou, X., Zhou, Y., Zhai, Z., Chen, D., and Jiang, Z. (2009). ERIS, an endoplasmic reticulum IFN stimulator, activates innate immune signaling through dimerization. Proc. Natl. Acad. Sci. USA *106*, 8653–8658. https://doi.org/10.1073/pnas.0900850106.

8. Zhong, B., Yang, Y., Li, S., Wang, Y.Y., Li, Y., Diao, F., Lei, C., He, X., Zhang, L., Tien, P., and Shu, H.B. (2008). The adaptor protein MITA links virus-sensing receptors to IRF3 transcription factor activation. Immunity *29*, 538–550. https://doi.org/10.1016/j.immuni.2008.09.003.

9. Ishikawa, H., Ma, Z., and Barber, G.N. (2009). STING regulates intracellular DNA-mediated, type I interferon-dependent innate immunity. Nature *461*, 788–792. https://doi.org/10.1038/nature08476.

10. Li, X.D., Wu, J., Gao, D., Wang, H., Sun, L., and Chen, Z.J. (2013). Pivotal roles of cGAS-cGAMP signaling in antiviral defense and immune adjuvant effects. Science *341*, 1390–1394. https://doi.org/10.1126/science.1244040.

11. Sun, L., Wu, J., Du, F., Chen, X., and Chen, Z.J. (2013). Cyclic GMP-AMP synthase is a cytosolic DNA sensor that activates the type I interferon pathway. Science *339*, 786–791. https://doi.org/10.1126/science.1232458.

12. Wu, J., Sun, L., Chen, X., Du, F., Shi, H., Chen, C., and Chen, Z.J. (2013). Cyclic GMP-AMP is an endogenous second messenger in innate immune signaling by cytosolic DNA. Science *339*, 826–830. https://doi.org/10.1126/science.1229963.

13. Krasteva, P.V., and Sondermann, H. (2017). Versatile modes of cellular regulation via cyclic dinucleotides. Nat. Chem. Biol. *13*, 350–359. https://doi.org/10.1038/nchembio.2337.

14. Gutjahr, A., Papagno, L., Nicoli, F., Kanuma, T., Kuse, N., Cabral-Piccin, M.P., Rochereau, N., Gostick, E., Lioux, T., Perouzel, E., et al. (2019). The STING ligand cGAMP potentiates the efficacy of vaccine-induced CD8+ T cells. JCI Insight *4*, e125107. https://doi.org/10.1172/jci.insight.125107.

15. Kuse, N., Sun, X., Akahoshi, T., Lissina, A., Yamamoto, T., Appay, V., and Takiguchi, M. (2019). Priming of HIV-1-specific CD8(+) T cells with strong functional properties from naive T cells. EBioMedicine *42*, 109–119. https://doi.org/10.1016/j.ebiom.2019.03.078.

16. Gray, P.M., Forrest, G., Wisniewski, T., Porter, G., Freed, D.C., DeMartino, J.A., Zaller, D.M., Guo, Z., Leone, J., Fu, T.M., and Vora, K.A. (2012). Evidence for cyclic diguanylate as a vaccine adjuvant with novel immunostimulatory activities. Cell. Immunol. *278*, 113–119. https://doi.org/10.1016/j.cellimm.2012.07.006.

17. Morehouse, B.R., Govande, A.A., Millman, A., Keszei, A.F.A., Lowey, B., Ofir, G., Shao, S., Sorek, R., and Kranzusch, P.J. (2020). STING cyclic dinucleotide sensing originated in bacteria. Nature *586*, 429–433. https://doi.org/10.1038/s41586-020-2719-5.

18. Cavlar, T., Deimling, T., Ablasser, A., Hopfner, K.P., and Hornung, V. (2013). Species-specific detection of the antiviral small-molecule compound CMA by STING. EMBO J. *32*, 1440–1450. https://doi.org/10.1038/emboj.2013.86.

19. Gao, P., Ascano, M., Zillinger, T., Wang, W., Dai, P., Serganov, A.A., Gaffney, B.L., Shuman, S., Jones, R.A., Deng, L., et al. (2013). Structure-function analysis of STING activation by c[G(2', 5')pA(3', 5')p] and targeting by antiviral DMXAA. Cell *154*, 748–762. https://doi.org/10.1016/j.cell.2013.07.023.

20. Corrales, L., Glickman, L.H., McWhirter, S.M., Kanne, D.B., Sivick, K.E., Katibah, G.E., Woo, S.R., Lemmens, E., Banda, T., Leong, J.J., et al. (2015). Direct activation of STING in the tumor microenvironment leads to potent and systemic tumor regression and immunity. Cell Rep. *11*, 1018–1030. https://doi.org/10.1016/j.celrep.2015.04.031.

21. Miller, B.C., Sen, D.R., Al Abosy, R., Bi, K., Virkud, Y.V., LaFleur, M.W., Yates, K.B., Lako, A., Felt, K., Naik, G.S., et al. (2019). Subsets of exhausted CD8(+) T cells differentially mediate tumor control and respond to checkpoint blockade. Nat. Immunol. *20*, 326–336. https://doi.org/10.1038/s41590-019-0312-6.

22. Siddiqui, I., Schaeuble, K., Chennupati, V., Fuertes Marraco, S.A., Calderon-Copete, S., Pais Ferreira, D., Carmona, S.J., Scarpellino, L., Gfeller, D., Pradervand, S., et al. (2019). Intratumoral tcf1(+)PD-1(+)CD8(+) T cells with stem-like properties promote tumor control in response to vaccination and checkpoint blockade immunotherapy. Immunity *50*, 195–211.e10. https://doi.org/10.1016/j.immuni.2018.12.021.

23. Le Naour, J., Zitvogel, L., Galluzzi, L., Vacchelli, E., and Kroemer, G. (2020). Trial watch: STING agonists in cancer therapy. Oncoimmunology *9*, 1777624. https://doi.org/10.1080/2162402X.2020.1777624.

24. Konno, H., Konno, K., and Barber, G.N. (2013). Cyclic dinucleotides trigger ULK1 (ATG1) phosphorylation of STING to prevent sustained innate immune signaling. Cell *155*, 688–698. https://doi.org/10.1016/j.cell.2013.09.049.

25. Ahn, J., Gutman, D., Saijo, S., and Barber, G.N. (2012). STING manifests self DNA-dependent inflammatory disease. Proc. Natl. Acad. Sci. USA *109*, 19386–19391. https://doi.org/10.1073/pnas.1215006109.

26. Gall, A., Treuting, P., Elkon, K.B., Loo, Y.M., Gale, M., Jr., Barber, G.N., and Stetson, D.B. (2012). Autoimmunity initiates in nonhematopoietic cells and progresses via lymphocytes in an interferon-dependent autoimmune disease. Immunity *36*, 120–131. https://doi.org/10.1016/j.immuni.2011.11.018.

27. Jeremiah, N., Neven, B., Gentili, M., Callebaut, I., Maschalidi, S., Stolzenberg, M.C., Goudin, N., Frémond, M.L., Nitschke, P., Molina, T.J., et al. (2014). Inherited STING-activating mutation underlies a familial inflammatory syndrome with lupus-like manifestations. J. Clin. Invest. *124*, 5516–5520. https://doi.org/10.1172/JCI79100.

28. König, N., Fiehn, C., Wolf, C., Schuster, M., Cura Costa, E., Tüngler, V., Alvarez, H.A., Chara, O., Engel, K., Goldbach-Mansky, R., et al. (2017). Familial chilblain lupus due to a gain-of-function mutation in STING. Ann. Rheum. Dis. *76*, 468–472. https://doi.org/10.1136/annrheumdis-2016-209841.

29. Liu, Y., Jesus, A.A., Marrero, B., Yang, D., Ramsey, S.E., Sanchez, G.A.M., Tenbrock, K., Wittkowski, H., Jones, O.Y., Kuehn, H.S., et al. (2014). Activated STING in a vascular and pulmonary syndrome. N. Engl. J. Med. *371*, 507–518. https://doi.org/10.1056/NEJMoa1312625.

30. Ramanjulu, J.M., Pesiridis, G.S., Yang, J., Concha, N., Singhaus, R., Zhang, S.Y., Tran, J.L., Moore, P., Lehmann, S., Eberl, H.C., et al. (2018). Design of amidobenzimidazole STING receptor agonists with systemic activity. Nature *564*, 439–443. https://doi.org/10.1038/s41586-018-0705-y.

31. Palermo, R.E., Tisoncik-Go, J., Korth, M.J., and Katze, M.G. (2013). Old world monkeys and new age science: the evolution of non-human primate systems virology. ILAR J. *54*, 166–180. https://doi.org/10.1093/ilar/ilt039.

32. Shen, S., Pyo, C.W., Vu, Q., Wang, R., and Geraghty, D.E. (2013). The essential detail: the genetics and genomics of the primate immune response. ILAR J. *54*, 181–195. https://doi.org/10.1093/ilar/ilt043.

33. Donnelly, C.R., Jiang, C., Andriessen, A.S., Wang, K., Wang, Z., Ding, H., Zhao, J., Luo, X., Lee, M.S., Lei, Y.L., et al. (2021). STING controls nociception via type I interferon signalling in sensory neurons. Nature *591*, 275–280. https://doi.org/10.1038/s41586-020-03151-1.

34. Liu, Z., Zhou, J., Xu, W., Deng, W., Wang, Y., Wang, M., Wang, Q., Hsieh, M., Dong, J., Wang, X., et al. (2022). A novel STING agonist-adjuvanted pan-sarbecovirus vaccine elicits potent and durable neutralizing antibody and T cell responses in mice, rabbits and NHPs. Cell Res. *32*, 269–287. https://doi.org/10.1038/s41422-022-00612-2.

35. Masuta, Y., Yamamoto, T., Natsume-Kitatani, Y., Kanuma, T., Moriishi, E., Kobiyama, K., Mizuguchi, K., Yasutomi, Y., and Ishii, K.J. (2018). An antigen-free, plasmacytoid dendritic cell-targeting immunotherapy to bolster memory CD8(+) T cells in nonhuman primates. J. Immunol. *200*, 2067–2075. https://doi.org/10.4049/jimmunol.1701183.

36. van der Kuyl, A.C., van den Burg, R., Zorgdrager, F., Groot, F., Berkhout, B., and Cornelissen, M. (2007). Sialoadhesin (CD169) expression in CD14+ cells is upregulated early after HIV-1 infection and increases during disease progression. PLoS One *2*, e257. https://doi.org/10.1371/journal.pone.0000257.

37. Affandi, A.J., Olesek, K., Grabowska, J., Nijen Twilhaar, M.K., Rodríguez, E., Saris, A., Zwart, E.S., Nossent, E.J., Kalay, H., de Kok, M., et al. (2021). CD169 defines activated CD14(+) monocytes with enhanced CD8(+) T cell activation capacity. Front. Immunol. *12*, 697840. https://doi.org/10.3389/fimmu.2021.697840.

38. Lutz, C.T., Karapetyan, A., Al-Attar, A., Shelton, B.J., Holt, K.J., Tucker, J.H., and Presnell, S.R. (2011). Human NK cells proliferate and die in vivo more rapidly than T cells in healthy young and elderly adults. J. Immunol. *186*, 4590–4598. https://doi.org/10.4049/jimmunol.1002732.

39. Huang, L., Li, L., Lemos, H., Chandler, P.R., Pacholczyk, G., Baban, B., Barber, G.N., Hayakawa, Y., McGaha, T.L., Ravishankar, B., et al. (2013). Cutting edge: DNA sensing via the STING adaptor in myeloid dendritic cells induces potent tolerogenic responses. J. Immunol. *191*, 3509–3513. https://doi.org/10.4049/jimmunol.1301419.

40. Franceschi, C., Monti, D., Barbieri, D., Grassilli, E., Troiano, L., Salvioli, S., Negro, P., Capri, M., Guido, M., Azzi, R., et al. (1995). Immunosenescence in humans: deterioration or remodelling? Int. Rev. Immunol. *12*, 57–74. https://doi.org/10.3109/08830189509056702.

41. Fali, T., Fabre-Mersseman, V., Yamamoto, T., Bayard, C., Papagno, L., Fastenackels, S., Zoorab, R., Koup, R.A., Boddaert, J., Sauce, D., and Appay, V. (2018). Elderly human hematopoietic progenitor cells express cellular senescence markers and are more susceptible to pyroptosis. JCI Insight *3*, e95319. https://doi.org/10.1172/jci.insight.95319.

42. Dunn, G.P., Old, L.J., and Schreiber, R.D. (2004). The immunobiology of cancer immunosurveillance and immunoediting. Immunity *21*, 137–148. https://doi.org/10.1016/j.immuni.2004.07.017.

43. Shankaran, V., Ikeda, H., Bruce, A.T., White, J.M., Swanson, P.E., Old, L.J., and Schreiber, R.D. (2001). IFNgamma and lymphocytes prevent primary tumour development and shape tumour immunogenicity. Nature *410*, 1107–1111. https://doi.org/10.1038/35074122.

44. Dunn, G.P., Bruce, A.T., Sheehan, K.C.F., Shankaran, V., Uppaluri, R., Bui, J.D., Diamond, M.S., Koebel, C.M., Arthur, C., White, J.M., and Schreiber, R.D. (2005). A critical function for type I interferons in cancer immunoediting. Nat. Immunol. *6*, 722–729. https://doi.org/10.1038/ni1213.

45. Zitvogel, L., Galluzzi, L., Kepp, O., Smyth, M.J., and Kroemer, G. (2015). Type I interferons in anticancer immunity. Nat. Rev. Immunol. *15*, 405–414. https://doi.org/10.1038/nri3845.

46. Klarquist, J., Hennies, C.M., Lehn, M.A., Reboulet, R.A., Feau, S., and Janssen, E.M. (2014). STING-mediated DNA sensing promotes antitumor and autoimmune responses to dying cells. J. Immunol. *193*, 6124–6134. https://doi.org/10.4049/jimmunol.1401869.

47. Woo, S.R., Fuertes, M.B., Corrales, L., Spranger, S., Furdyna, M.J., Leung, M.Y.K., Duggan, R., Wang, Y., Barber, G.N., Fitzgerald, K.A., et al. (2014). STING-dependent cytosolic DNA sensing mediates innate immune recognition of immunogenic tumors. Immunity *41*, 830–842. https://doi.org/10.1016/j.immuni.2014.10.017.

48. Guilliams, M., Ginhoux, F., Jakubzick, C., Naik, S.H., Onai, N., Schraml, B.U., Segura, E., Tussiwand, R., and Yona, S. (2014). Dendritic cells, monocytes and macrophages: a unified nomenclature based on ontogeny. Nat. Rev. Immunol. *14*, 571–578. https://doi.org/10.1038/nri3712.

49. Bode, C., Fox, M., Tewary, P., Steinhagen, A., Ellerkmann, R.K., Klinman, D., Baumgarten, G., Hornung, V., and Steinhagen, F. (2016). Human plasmacytoid dentritic cells elicit a Type I Interferon response by sensing DNA via the cGAS-STING signaling pathway. Eur. J. Immunol. *46*, 1615–1621. https://doi.org/10.1002/eji.201546113.

50. Hervas-Stubbs, S., Riezu-Boj, J.I., Mancheño, U., Rueda, P., Lopez, L., Alignani, D., Rodríguez-García, E., Thieblemont, N., and Leclerc, C. (2014). Conventional but not plasmacytoid dendritic cells foster the systemic virus-induced type I IFN response needed for efficient CD8 T cell priming. J. Immunol. *193*, 1151–1161. https://doi.org/10.4049/jimmunol.1301440.

51. Shimasaki, N., Jain, A., and Campana, D. (2020). NK cells for cancer immunotherapy. Nat. Rev. Drug Discov. *19*, 200–218. https://doi.org/10.1038/s41573-019-0052-1.

52. Marcus, A., Mao, A.J., Lensink-Vasan, M., Wang, L., Vance, R.E., and Raulet, D.H. (2018). Tumor-derived cGAMP triggers a STING-mediated interferon response in non-tumor cells to activate the NK cell response. Immunity *49*, 754–763.e4. https://doi.org/10.1016/j.immuni.2018.09.016.

53. McFarland, A.P., Luo, S., Ahmed-Qadri, F., Zuck, M., Thayer, E.F., Goo, Y.A., Hybiske, K., Tong, L., and Woodward, J.J. (2017). Sensing of bacterial cyclic dinucleotides by the oxidoreductase RECON promotes NF-kappaB activation and shapes a proinflammatory antibacterial state. Immunity *46*, 433–445. https://doi.org/10.1016/j.immuni.2017.02.014.

54. Li, W., Lu, L., Lu, J., Wang, X., Yang, C., Jin, J., Wu, L., Hong, X., Li, F., Cao, D., et al. (2020). cGAS-STING-mediated DNA sensing maintains CD8(+) T cell stemness and promotes antitumor T cell therapy. Sci. Transl. Med. *12*, eaay9013. https://doi.org/10.1126/scitranslmed.aay9013.

55. Deb, P., Dai, J., Singh, S., Kalyoussef, E., and Fitzgerald-Bocarsly, P. (2020). Triggering of the cGAS-STING pathway in human plasmacytoid dendritic cells inhibits TLR9-mediated IFN production. J. Immunol. *205*, 223–236. https://doi.org/10.4049/jimmunol.1800933.

56. Tang, C.H.A., Zundell, J.A., Ranatunga, S., Lin, C., Nefedova, Y., Del Valle, J.R., and Hu, C.C.A. (2016). Agonist-mediated activation of STING induces apoptosis in malignant B cells. Cancer Res. *76*, 2137–2152. https://doi.org/10.1158/0008-5472.CAN-15-1885.

57. Pulendran, B. (2009). Learning immunology from the yellow fever vaccine: innate immunity to systems vaccinology. Nat. Rev. Immunol. *9*, 741–747. https://doi.org/10.1038/nri2629.

58. HIPC-CHI Signatures Project Team; HIPC-I Consortium (2017). Multicohort analysis reveals baseline transcriptional predictors of influenza vaccination responses. Sci. Immunol. *2*, eaal4656. https://doi.org/10.1126/sciimmunol.aal4656.

59. Metcalf, T.U., Cubas, R.A., Ghneim, K., Cartwright, M.J., Grevenynghe, J.V., Richner, J.M., Olagnier, D.P., Wilkinson, P.A., Cameron, M.J., Park, B.S., et al. (2015). Global analyses revealed age-related alterations in innate immune responses after stimulation of pathogen recognition receptors. Aging Cell *14*, 421–432. https://doi.org/10.1111/acel.12320.

60. Bruel, T., Dupuy, S., Démoulins, T., Rogez-Kreuz, C., Dutrieux, J., Corneau, A., Cosma, A., Cheynier, R., Dereuddre-Bosquet, N., Le Grand, R., and Vaslin, B. (2014). Plasmacytoid dendritic cell dynamics tune interferon-alfa production in SIV-infected cynomolgus macaques. PLoS Pathog. *10*, e1003915. https://doi.org/10.1371/journal.ppat.1003915.

61. Lee, M.Y.H., Upadhyay, A.A., Walum, H., Chan, C.N., Dawoud, R.A., Grech, C., Harper, J.L., Karunakaran, K.A., Nelson, S.A., Mahar, E.A., et al. (2021). Tissue-specific transcriptional profiling of plasmacytoid dendritic cells reveals a hyperactivated state in chronic SIV infection. PLoS Pathog. *17*, e1009674. https://doi.org/10.1371/journal.ppat.1009674.

62. Price, J.L., Manetz, T.S., Shearer, J.D., and House, R.V. (2013). Preclinical safety assessment of a recombinant plague vaccine (rF1V). Int. J. Toxicol. *32*, 327–335. https://doi.org/10.1177/1091581813497405.